EXAFS and DRIFTS study of lanthanide doped rhodium catalysts☆

P. Malet, J.J. Benitez, M.J. Capitan, M.A.Centeno, I.Carrizosa and J.A. Odriozola

Departamento de Quimica Inorganica e Instituto de Ciencia de Materiales de Sevilla, Centro Mixto Universidad de Sevilla-CSIC, PO Box 874, 41080 Sevilla, Spain

Received 19 June 1992; accepted 11 January 1993

The activity for the production of methane in the hydrogenation of carbon oxides has been measured over rare earth oxide (Ln = La, Ce, Sm, Yb, Lu) promoted Rh/Al_2O_3 catalysts in a fixed bed flow reactor at atmospheric pressure. The catalyst structures have been determined by EXAFS experiments at the K edge of the rhodium metal. From the EXAFS data it is concluded that the average coordination number of rhodium depends on the rare earth cation used as promoter. The Rh average coordination number follows the trend obtained from CO chemisorption data. The correlation of the activity results with the structural data demonstrates that the activity towards methane production decreases on increasing the metal dispersion, this being the main effect the promoter causes on the rhodium catalyst.

Keywords: CO hydrogenation by rhodium; EXAFS study of rhodium

1. Introduction

Promoters exert a significant influence on the activity and selectivity of catalysts in the hydrogenation of carbon oxides, especially over the diagonal elements of group VIII metals, in which they may drive the reaction towards the production of hydrocarbons or oxygenates selectively [1].

The promoter effect may be associated to electronic, by changing the metal work function, or geometric effects either by modifying the metal dispersion or the particle shape or by migrating on top of the metal particle giving rise to a decorating effect [2].

The effect of rare earth promoters on the hydrogenation of carbon oxides has been described over several metals [3–12]. However, the results reported are far from being coincident. Thus, Rieck and Bell [3] studying Pd catalysts reported that

☆ Paper presented at the 203rd ACS National Meeting, Surface Science and Catalysis: Students and Friends of G.A. Somorjai (San Francisco 1992).

rare earth oxides do not influence the activity towards methane, although the formation of LaO_x on top of the metal crystallites favours the formation of methanol, in this way decreasing the selectivity to CH_4. This geometric effect has also been reported for Rh/La_2O_3 systems by Bernal et al. [4], who found the migration of the support over the Rh particle.

Recently, Barrault and Alouche [6] found that Ce or La promotion of Ni catalysts resulted in a decrease of the activity for methane production. Besides, several studies proposed that rare earth supported on alumina acts as a dispersant for added metals [13,14]. If this is the case, an increase of the metal dispersion due to the presence of rare earths should result in an activity decrease as reported by Barrault and Alouche [6] and would match the CH_4 production scheme reported by Mori et al. [15] for Rh/Al_2O_3 catalysts. On the contrary, Ichikawa et al. [11] and Doering et al. [12] found that the activity in CH_4 production increases on increasing the metal dispersion.

These contradictory results might be associated to the difficulty in measuring the metal dispersion by CO and H_2 chemisorption, since the adsorption stoichiometry can vary and the adsorbates may interact with the substrate support [16,17].

In this work, we study the promoter effect of rare earth oxides on Rh/Al_2O_3 catalysts in the hydrogenation of carbon oxides. Besides the conventional measure of the dispersion by chemisorption of probe molecules EXAFS experiments on the reduced catalysts are carried out. The obtained metal dispersion is then correlated to activity results.

2. Experimental

An impregnation method was followed for preparing all the supports described in this work. Gamma alumina (Degussa, type C) was used as support. Lanthanide oxide (Ln = La, Ce, Sm, Yb, Lu) (Sigma Chemical Co., 99.99% pure) was dissolved in 4 M HNO_3 (Merck, a.r. grade). A solution amount sufficient for obtaining a 10% w/w (100Ln/Ln + Al = 3.5) lanthanide oxide on alumina was added to a beaker in which the alumina powder had been placed. The slurry thus prepared was continuously stirred and heated to 60–70°C until the solvent was eliminated. Once the solvent evaporated the resulting solid was oven dried overnight (110°C) and crushed in an agata mortar. The supports were prepared by calcining the solids for four hours at 600°C. The supports prepared are free from nitrate species as confirmed by TPD.

The catalysts were prepared by incipient wetness from rhodium nitrate solutions (Ventron). For obtaining the desired rhodium loading (1% w/w) six successive impregnation cycles at room temperature were needed. The catalyst precursor was then oven dried overnight at 110°C.

The catalyst precursor was reduced in situ shortly before running experiments. The precursor, placed in the reaction cell, was ramped in temperature up to 350°C, in the presence of O_2. The oxidizing atmosphere was kept at this temperature for 1 h and then the O_2 flow replaced by He. Once all the oxygen was removed, a H_2 flow was

admitted into the reaction chamber which was maintained in an isothermal condition for 1 h. This treatment leads to the formation of Rh^0 species as stated by XPS [7].

The specific surface area of the catalysts was measured in a conventional oil diffusion pumped glass system and resulted in 95 5 $m^2\ g^{-1}$ in every case.

Diffuse reflectance infrared Fourier transform spectroscopy (DRIFTS) was carried out in a Nicolet 5DXE spectrometer with a resolution of 4 cm^{-1}. A reflectance cell (Spectra-Tech) that allows in situ treatments up to 500°C and 1 atm was coupled to the spectrometer. A reasonable signal-to-noise ratio was obtained by coadding 200 interferograms. Always, within this work, raw spectra are presented without smoothing or baseline corrections.

Catalytic tests were carried out in a stainless steel fixed bed flow reactor. The catalysts were placed between two stainless steel grids and the temperature measured by a K type thermocouple in close contact with the catalyst powder. A 1 : 3 CO_x : H_2 mixture was always fed into the reactor at a CO_x partial pressure of 0.08 atm and 20 ml min^{-1}. Product analysis was performed using on line GC (Hewlett-Packard 5834A). Data were taken after stabilizing the catalysts in the reaction mixture for 4 h at the highest reaction temperature (300°C) tried. Blank reaction test resulted in negligible amounts of CH_4.

EXAFS spectra were recorded at the L_{III} edge of lanthanum (5491 eV) and samarium (6716 eV), station DCI III at LURE (France); and at the Rh K edge (23228 eV) at station 9.2 at the SRS Daresbury Laboratory (UK). Monochromatization was obtained by a double silicon crystal working at the (311) reflection (LURE) and (220) reflection (Daresbury Laboratory). The measurements were carried out in transmission using optimized ion chambers as detectors. Support samples were pressed into self-supporting pellets with an absorbance of about 2.5, and measured at room temperature.

The rhodium spectra were measured at liquid nitrogen temperature in a cell which allows in situ treatments at temperatures up to 500°C and pressures of up to 1 atm.

The procedure for extracting and analyzing the EXAFS data has been previously described [18]. EXAFS data at Ln L_{III} edge were analyzed by using theoretically calculated Mac Kale's phase and backscattering amplitude functions [19] for the Ln–O and Ln–Ln contributions. EXAFS data at Rh K edge have been analyzed using experimental phase and amplitude functions for Rh–Rh and Rh–O contributions obtained from the EXAFS spectra of a rhodium foil and Rh_2O_3, respectively. Shell fitting in k and R spaces was done with application of both k^1 and k^3 weighting schemes, which results in a better decoupling of the coordination number (N) and the Debye–Waller factor ($\Delta\sigma^2$) as well as coordination distance (R) and inner potential correction (E_0) [20].

3. Results and discussion

The metallic dispersion has been measured by CO and H_2 chemisorption at room temperature (r.t.) assuming a CO/Rh ratio of 1 and a H_2/Rh ratio of 0.5, the

results obtained being shown in table 1. Dispersion values obtained from H_2 chemisorption can be affected by hydrogen spillover and non-dissociative adsorption effects that have been previously described for rhodium catalysts [21]. Besides this, dissociative adsorption at the support can take place. The dissociative chemisorption of H_2 over Ln_xO_y and Ln_xO_y/Al_2O_3 has been previously reported [16,22]. However, this latter hypothesis can be discarded since experiments carried over the support alone, at room temperature, result in a negligible amount of chemisorbed hydrogen.

In the case of the unpromoted catalyst in which the hydrogen spillover effect has been rejected [23], the H/Rh ratio may be representative of the actual dispersion of the catalyst. Moreover, the CO to H ratio, obtained from the results in table 1, is 1.2 which is in good agreement with the results of Cavanagh and Yates [24] for a 2.2% Rh/Al_2O_3 catalyst.

Among the promoted catalysts only the one promoted by La fails in producing a H/100Rh ratio above 100. However, if the reduction process is carried out at 450°C this parameter reaches a value of 111 for such a promoted catalyst. La_2O_3 undergoes, even at room temperature, a hydroxylation process that results in the formation of lanthanum hydroxide. Decomposition of this hydroxide occurs in two steps; the first one, at 350°C, results in the formation of LaO(OH) and the second one, at 450°C, in La_2O_3 [25]. If catalyst reduction takes place at 350°C the water produced in such a process may keep all the La cations hydroxylated, at higher reduction temperatures dehydroxylation takes place. H_2 adsorption at r.t. may then result in hydrogen spillover, explaining the results shown in table 1.

The extremely high dispersion value obtained, from H_2 chemisorption, for the Ce promoted catalyst should be explained considering the ability of CeO_2 for accommodating hydrogen within the lattice [26].

The metallic dispersion obtained from CO chemisorption is within the usually reported values for rhodium catalysts. However, CO can chemisorb on bridge/hollow sites or as gem-dicarbonyl species, that under- or overestimates the Rh dispersion [27]. Moreover, if the support and/or the promoter present a basic character the formation of carbonate species at the support can take place [17], overestimating again the metal dispersion.

When promoting Rh/Al_2O_3 catalysts with lanthanide oxides the presence of all types of carbonyl species is detected by FTIR. Fig. 1 shows the DRIFTS spectra of

Table 1
H_2 and CO adsorption on promoted $Rh/Al_{22}O_{33}$ catalysts

Promoter	H/100Rh	CO/100Rh
none	46	54
La_2O_3	97	62
CeO_2	753	51
Sm_2O_3	163	80
Yb_2O_3	110	96
Lu_2O_3	106	82

CO adsorbed on Rh/Al_2O_3 and Ln-promoted rhodium catalysts, at saturation coverage and r.t. For the non-promoted sample, bands at 2020 and 2093 cm^{-1} ascribed to gem-dicarbonyl species and a poorly resolved band at 2050 cm^{-1} that we ascribe to linear CO molecules [28] are observed. For the promoted catalysts bands at 2090, 2060 and 2020 cm^{-1} appear. In addition to this a new band at 1820 cm^{-1} that may be ascribed to bridge carbonyl species is present for all the promoted catalysts. However, this frequency is 50 to 80 wavenumbers lower than that reported by Hamadeh and Griffiths [28] for the stretching frequency of bridge carbonyls. An alternative description is related to the presence of carbonyl species bound to the support and the metal [29], which have been also claimed as responsible for the promoter effect of Ce in the hydrogenation of carbon oxides [30].

In addition to CO stretching bands the Ln-promoted catalysts present bands in the range 1600–1350 cm^{-1} that have to be ascribed to carbonate species [7,9]. It is worth of pointing out that, as lanthanum oxide is more basic than ytterbium oxide, the relative intensity of carbonate bands is smaller for the former than for the latter, which may indicate that CO interaction with the support occurs after reac-

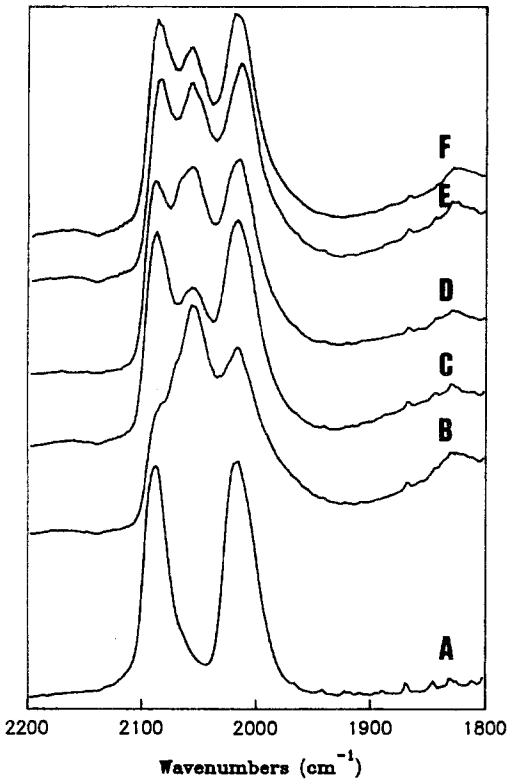

Fig. 1. DRIFTS spectra, at saturation coverage and room temperature, of CO adsorbed on Rh/Al_2O_3 (A), La-promoted (B), Ce-promoted (C), Sm-promoted (D), Yb-promoted (E) and Lu-promoted Rh/Al_2O_3 catalysts (F).

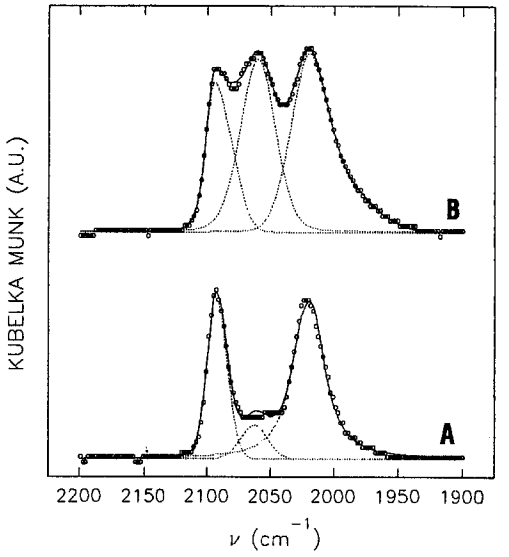

Fig. 2. Deconvoluted DRIFTS spectra of CO adsorbed on (A) Rh/Al_2O_3 and (B) Sm_2O_3-promoted Rh/Al_2O_3 catalysts.

tion on the metal surface. It has been pointed out by Castner et al. [31] that CO does not dissociate at the Rh(111) surface except at the defect sites but it dissociates at stepped surfaces. Erdohelyi and Solymosi [32] reported a CO dissociation below 1% for a 1% Rh/Al_2O_3 catalyst with H/Rh and CO/Rh ratios (0.33 and 0.35, respectively) similar to those shown in table 1. These literature data [31,32] suggest that the particle size is smaller for the Yb_2O_3-promoted catalyst than for the La_2O_3-promoted sample, resulting in a higher concentration of defect sites. The dissociation extent of the chemisorbed CO is within the experimental error and can be neglected for calculating the metal dispersion.

The complexity of the IR spectra in fig. 1 prevents the estimation of the amount of CO molecules corresponding to every type of interaction. However, in an attempt to estimate the ratio of the CO species adsorbed at the metal surface the deconvolution of the IR spectra in the 1900–2200 cm^{-1} region has been carried out. Fig. 2 shows the deconvoluted spectra in this region for the unpromoted and Sm_2O_3-promoted catalysts. The relative intensity of the bands at about 2020 and about 2090 cm^{-1} changes as a function of the angle formed by the two CO molecules. In our case, despite the apparent variation in intensity, the angle (2α) between the two CO dipoles using the relationship $A_{asym}/A_{sym} = \tan^2 \alpha$ is 110 10° for all the catalysts studied, in good agreement with the values reported by Rice et al. for Rh/Al_2O_3 catalysts [33]. In table 2 the intensity ratio between the gem-dicarbonyl ($A_{gem} = A_{2090} + A_{2020}$) and the linear CO species (A_{lin}) obtained after deconvoluting the IR spectra of the studied catalysts are shown. In fig. 3 the A_{gem} to A_{lin} ratio is plotted against the ionic potential ($\phi = Z/r$) of the cations present on the catalyst surface. It is clear that on increasing ϕ the A_{gem}/A_{lin} ratio increases.

Table 2
Gem-dicarbonyl-to-linear CO ratios calculated from the deconvoluted spectra

Promoter	None	La	Ce	Sm	Yb	Lu
A_{gem}/A_{lin}	10.464	1.300	2.722	1.939	1.999	2.002

The presence of the gem-dicarbonyl species is associated to the oxidation of Rh^0 species to Rh^+ cations due to the presence of OH groups on the alumina surface [34,35] according to

$$2Rh + 4CO + 2AlOH \rightarrow H_2 + 2Al{-}O{-}Rh(CO)_2.$$

This oxidation disrupts the Rh–Rh bonds generating the gem-dicarbonyl species. The result in fig. 3 can be explained by the interaction of the lanthanide cations with the hydroxyl groups of the alumina surface [18] which decreases surface OH acidity, changing the redox potential, leading to a lower concentration of the gem-species. A similar conclusion has been reached by silation of the hydroxyl groups of the Al_2O_3 [36].

As the formation of gem-dicarbonyl can be considered as a chemical attack of the acidic OH groups on the Rh particle coupled with the CO interaction, the presence of gem-CO species gives rise to uncertainty of the previous dispersion of the Rh particle.

Cavanagh and Yates [24] calculated the infrared extinction coefficient for gem-dicarbonyl species on a 0.2% Rh/Al_2O_3 catalyst assuming no contribution of linear CO species. They found $\epsilon = 13.8 \times 10^{-6}$ mol^{-1} cm whereas Duncan et al. [37] using NMR calculated $\epsilon = 202 \times 10^{-6}$ mol^{-1} cm for $Rh(CO)_2$ species. In addition to this, the extinction coefficient changes as the rhodium loading increases [24]. More

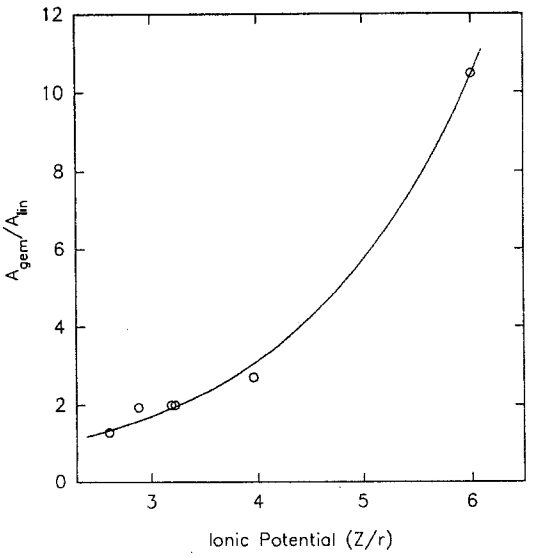

Fig. 3. Influence of the ionic potential of the cations at the support surface on the A_{gem}/A_{lin} ratio.

recently, Ballinger and Yates [38] stated the difficulty in determining the stoichiometry of the saturated CO/Rh and H/Rh layers for a 0.15% Rh/Al_2O_3 catalyst and postulated a high dispersion of the catalyst from IR data, but they did not try to establish the relative proportion of gem-to-linear species using the extinction coefficient previously calculated in Yates' group [24]. Estimations of the relative values of the extinction coefficients of CO on supported platinum have been published. So, it has been reported that the ratio of the extinction coefficient of linear CO to that of bridge CO is 4 to 13 [39]. These variabilities of the intensity ratios prevent the evaluation of the relative population of bridge, linear and gem-CO species even assuming that the extinction coefficients do not change on going from Pt to Rh.

If the rhodium particles expose the (111) face we can estimate the relative population of linear and bridge CO sites from the LEED and HREELS studies by Dubois and Somorjai [40]. They found at saturation coverages of CO on Rh(111) a (2×2) LEED pattern that can correspond to a unit cell consisting of three carbon monoxide molecules (two atop and one bridge), in good agreement with the two-to-one peak intensity ratio found by HREELS [40]. The LEED patterns for the CO adsorption on stepped surfaces (Rh(755) and Rh(331)) are quite similar to that found for the Rh(111) surface indicating that the CO structure is dominated by (111) terraces present in these surfaces [41]. So, a similar ratio of two-to-one linear to bridge site may be assumed for the case of small rhodium particles. However, it should be pointed out that the saturation coverage in rhodium single crystal is attained at 10^{-6} Torr [40]. At higher pressures, the surface unit cell may be compressed and the relative proportion of bridge-to-linear carbonyls may decrease.

By assuming that the area under the CO absorption curve corresponds exclusively to the gem-dicarbonyl species, for the Rh/Al_2O_3 catalyst, the proportion of gem-dicarbonyl species can be calculated in all the promoted catalysts (table 3). If the A_{gem}/A_{lin} obtained from the deconvolution of the DRIFTS spectrum for the Rh/Al_2O_3 catalysts corresponds to 100% gem-dicarbonyl species, such a ratio for the promoted catalysts should correspond to the fraction of gem-species in the promoted catalysts. For doing this it has to be considered that the extinction coefficient of the linear and gem-dicarbonyl species does not change on modifying the

Table 3
Relative amount of the different CO species adsorbed on the Rh particles from the deconvoluted DRIFTS spectra

Promoter	Gem- (%)	Linear (%)	Bridge (%)
none	100[a]	–	–
La	7.65	61.56	30.79
Ce	14.78	56.81	28.41
Sm	11.00	59.34	29.66
Yb	11.30	59.14	29.56
Lu	11.31	59.13	29.56

[a] Assumed value.

promoter. The relative proportion of bridge-to-linear CO species has been kept constant according to the LEED data published for rhodium single crystals [40,41]. While this is not a strictly correct procedure where mixtures of chemisorbed CO species are involved, the method yields an index of gem-dicarbonyl species which is of qualitative value along the series of promoted catalysts.

Taking for granted both assumptions, (i) 100% of the carbonyl species are present as gem-dicarbonyl in the unpromoted catalyst, and (ii) the surface unit cell consists of two linear CO and one bridge, the relative amount of different CO species has been calculated (table 3). It is clear, that for the promoted catalysts the relative proportion of the gem-to-linear-to-bridge CO species remains practically constant. In consequence, the CO/100Rh ratios calculated from chemisorption data are representative of the trend of actual dispersions. Even, if the proportion of gem-dicarbonyl species in the unpromoted catalyst were lower than 100%, as it should be, the observed trend for the promoted catalysts would not change. However, it is hardly possible to obtain absolute values for the metal dispersions from the DRIFTS spectra of chemisorbed CO.

As the observed DRIFTS spectrum for the Rh/Al_2O_3 is the result of the reaction of the rhodium particles with the acid protons of the support in the presence of CO [34,35], conclusions on the metal dispersion cannot be driven from the DRIFTS data. So, establishing of the actual dispersion from the CO and H_2 chemisorption data, and the infrared spectra of adsorbed CO is far from being straightforward. However, all the reported data suggest that the CO/100Rh ratio (table 1) may be representative of the trend of the actual dispersion values for the promoted catalysts. However, no reliable information is obtained for the unpromoted catalyst.

Fig. 4 shows the turnover frequencies (TOF) for methane production in the hydrogenation of CO and CO_2 over the series of catalysts studied as a function of the CO/100Rh ratio. The TOF in the hydrogenation of CO_2 is higher than in the case of CO, as previously reported for Rh/Al_2O_3 catalysts [42].

As methane production occurs at the metal crystallites by hydrogenating the carbonaceous residue [15] two possibilities can be considered for the regular trend observed in fig. 4: (i) the metal work function is affected by the presence of lanthanide cations hindering CO dissociation which results in a decrease in the turnover frequency and (ii) lanthanide cations modify the acid–base character of the surface resulting in altering the metal dispersion, which is the major effect on the turnover frequency.

Promoting Rh catalysts with potassium the metal work function is lowered and the dissociation of CO is attained easily [43]. CO stretching bands in the K-doped catalysts present a shift towards lower wavenumbers that justifies such an interpretation [44]. In our case the CO stretching frequency remains constant whatever the lanthanide promoter added. The first explanation can then be disregarded.

Concerning the second hypothesis a confirmation of the trend of the CO chemisorption results should be obtained, especially for the unpromoted catalyst for

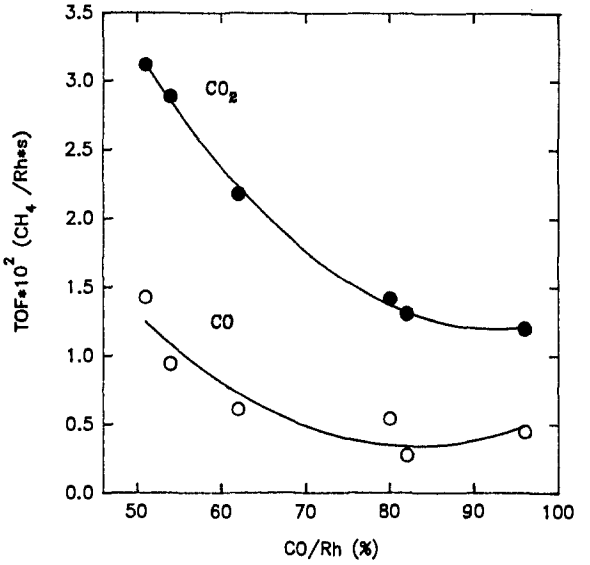

Fig. 4. Turnover frequencies for the hydrogenation of CO_x, at 270°C and 1 atm, over H_2-reduced Rh/Al_2O_3 catalysts.

which the difficulty of obtaining valuable information from the DRIFTS spectrum has been demonstrated. For doing this, EXAFS analyses of the rhodium K edge have been performed on Rh/Al_2O_3 and La- and Sm-promoted catalysts, the first one as a control system and the promoted samples as representatives of systems with low and high CO/Rh ratios.

The X-ray absorption spectrum of rhodium catalysts have been taken in situ after heating in He flow at 350°C and further reduction in H_2 flow. The absence of the white line in the H_2 treated samples confirms the reduction of the catalysts.

The EXAFS function for the promoted and unpromoted catalysts is shown in fig. 5 for both the He- and H_2-treated catalysts, and the FT in fig. 6. For the reduced catalysts only one peak at 2.2 Å without phase and backscattering amplitude correction is appreciable for all the catalysts; this peak corresponds to Rh–Rh scatterer pairs indicating the complete reduction of the catalysts. In all cases the spectrum is quite well reproduced introducing a single rhodium shell, dotted line in figs. 5 and 6, at $R = 2.68$ Å after phase and backscattering amplitude correction which reproduces the Rh–Rh distance in the bulk crystal [34]. It is important to notice that the fitting is attained without introducing the presence of lanthanide cations and/or a second rhodium shell, table 4. Alternative fittings introducing shells at $R\sqrt{2}$ or $R\sqrt{3}$, which accounts for different particle shapes, have been tried; in neither case a reasonable set of parameters was obtained. Tamura and Nihei [45] have proposed from photoelectron diffraction of Rh clusters deposited on the (0001) plane of α-Al_2O_3 the formation of the rhodium particles consisting of 13 atoms (fig. 7). Van 't Blik et al. [34] studied the structure of rhodium

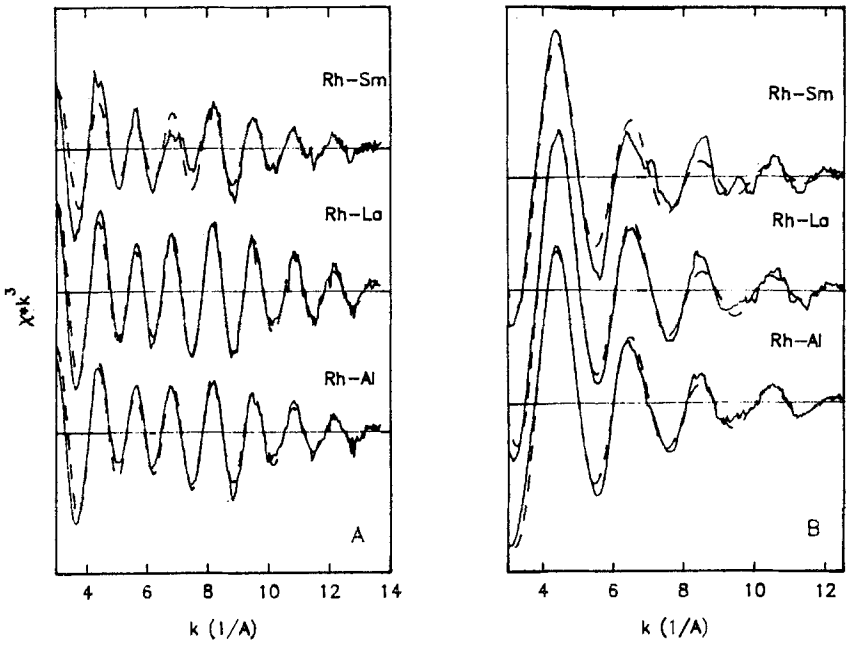

Fig. 5. EXAFS function, at the rhodium K edge, for Rh/Al_2O_3 and La- and Sm-promoted Rh/Al_2O_3 catalysts. (A) H_2-reduced catalysts. (B) Precursor decomposed in He at 350°C. Solid lines: unfiltered oscillatory function. Dotted lines: fitted spectra.

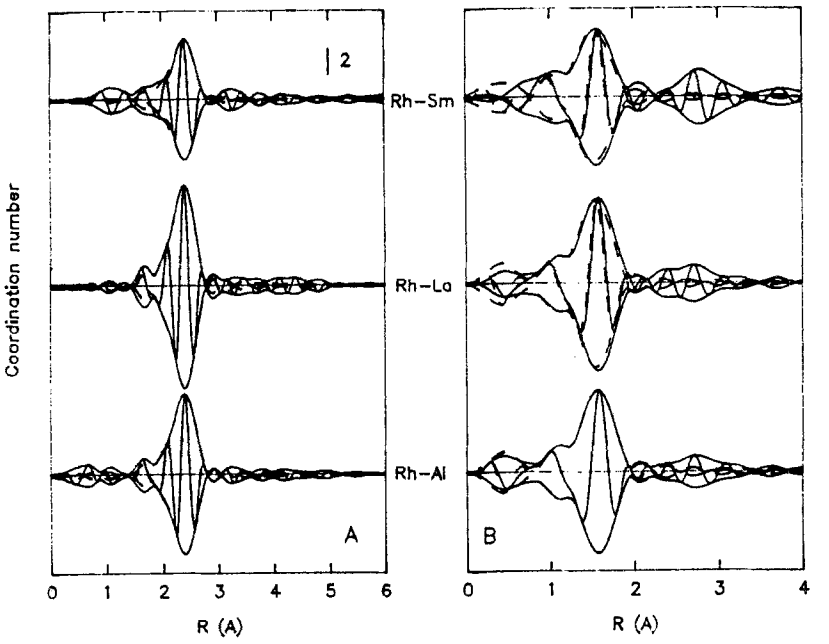

Fig. 6. Fourier transform in k^3-weighting of the rhodium EXAFS function for Rh/Al_2O_3 and La- and Sm-promoted Rh/Al_2O_3 catalysts. (A) H_2-reduced catalysts. (B) Precursor decomposed in He at 350°C. Solid lines: raw data. Dotted lines: fitted spectra.

Table 4
EXAFS parameter values for H_2-reduced $Rh/Al_{22}O_{33}$ catalysts

Promoter	N	R(Å)	$\Delta\sigma^2$ (Å^2)
none	6.4_4	2.67_8	0.00564
La_2O_3	6.5_8	2.68_0	0.00462
Sm_2O_3	4.6_7	2.68_2	0.00562

(0.57% Rh/Al_2O_3) by determining the coordination of Rh atoms by EXAFS. They found the metal crystallites consist of 15–20 atoms clusters.

If we assume the Tamura and Nihei's particle as representative of the Rh clusters the average coordination number for rhodium would be 5, and the metal dispersion, considering one CO molecule per Rh site of 1, of about 95%. This result fits the CO/Rh ratio calculated from chemisorption data for the Yb_2O_3-promoted catalyst (table 1). The coordination number of rhodium from the fitting of the EXAFS function for the Sm-promoted catalyst (CO/Rh = 0.80) is close to the value calculated for the particle described by Tamura and Nihei [45], and also fits the coordination number obtained by EXAFS by Van 't Blik et al. (N = 3.7 0.6) on a 0.57% Rh/Al_2O_3 catalyst [34]; so, a particle consisting of 15–20 atoms can be envisaged for this catalyst.

Although the exact shape of the metal particles cannot be obtained from EXAFS experiments and in consequence the metal dispersion cannot be exactly calculated from the coordination numbers in table 4, the observed trend in coordination numbers, higher for the less disperse catalysts, follows the CO/100Rh trend obtained from CO chemisorption (table 1). Besides this, it can be stressed that the average coordination number for rhodium in the unpromoted and the La_2O_3-promoted catalysts is similar validating the CO/100Rh ratio obtained from chemisorption data.

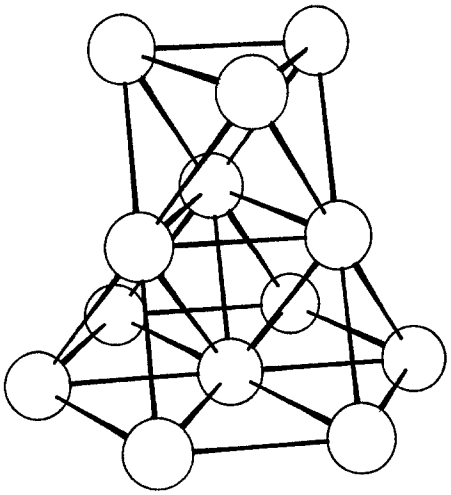

Fig. 7. Rhodium particle model for Yb-promoted Rh/Al_2O_3 catalyst.

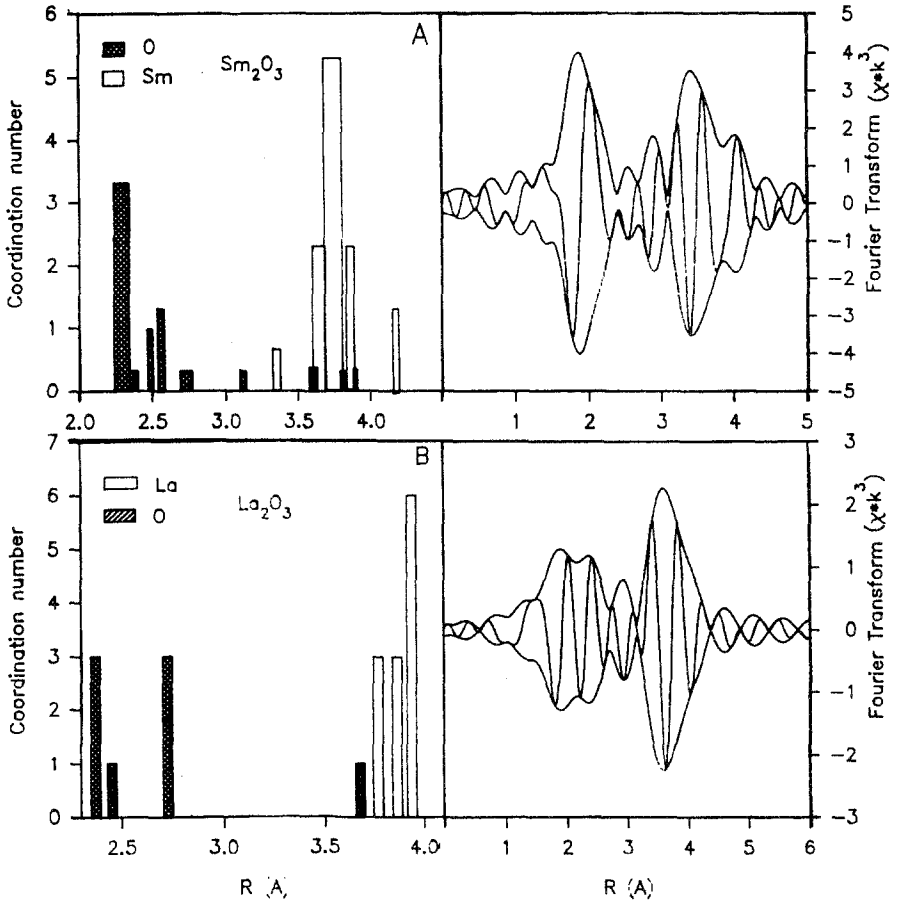

Fig. 8. Radial distribution function and experimental FTs in k^3-weighting for Ln_2O_3 reference compounds.

The FT of the EXAFS function for the He heated catalysts presents two peaks without phase and backscattering amplitude correction at $R = 1.5$ and 2.7 Å that can be ascribed to Rh–O and Rh–Rh scatterer pairs in RhO_x. Although the peak at $R = 2.7$ Å increases in intensity on going from the unpromoted to La- and Sm-promoted catalysts (fig. 6), its position remains constant whatever the promoter used. This let us discard it is due to Rh–Ln scatterer pairs then eliminating the possibility of knowing the relative position of the rhodium cluster with respect to the lanthanide promoter.

In an attempt to obtain information of the relative situation of the rhodium particles and the lanthanide promoter, X-ray absorption experiments have been carried out at the lanthanide edges.

The structure of the Ln_2O_3/Al_2O_3 supports has been also studied by EXAFS at the L_{III} edge of the lanthanide cations. The EXAFS analysis is limited in the most favourable case to about 600 eV since the appearance of the L_{II} edge of the lantha-

nide cation. According to the number of independent data points available the maximum number of coordination shells that can be fitted is five [18]. Since the radial distribution function (RDF) around the lanthanide cation is quite complex, an analysis of reference compounds should be performed. Fig. 8 shows the RDF of La_2O_3 and Sm_2O_3 and the Fourier transform in k-weighting three of the EXAFS functions of the lanthanide oxides studied in this work. Except for the lanthanum oxide there is quite a good agreement between the calculated parameters and the experimental results from X-ray diffraction. In the case of lanthanum oxide the number of lanthanum cations present in the second coordination shell is too low, which might indicate that the oxide reacts with the surrounding atmosphere undergoing hydration, which results in the formation of an hydroxide with a smaller average number of lanthanum cations [25].

Fig. 9 shows the unfitted oscillatory EXAFS functions as a function of wavenumber k of the L_{III} edges of the lanthanide cations and the corresponding k^3-weighted FT. For the La- and Sm-promoted supports a main peak in the FT at about $R = 2.0$ Å can be observed while peaks corresponding to higher coordination shells are absent. By comparing these FT with those corresponding to the reference compounds this peak should be ascribed to Ln–O scatterer pairs.

Following the fitting procedure described in the experimental section the coordination number and bond distances around the lanthanide cations in the supports are obtained (table 5).

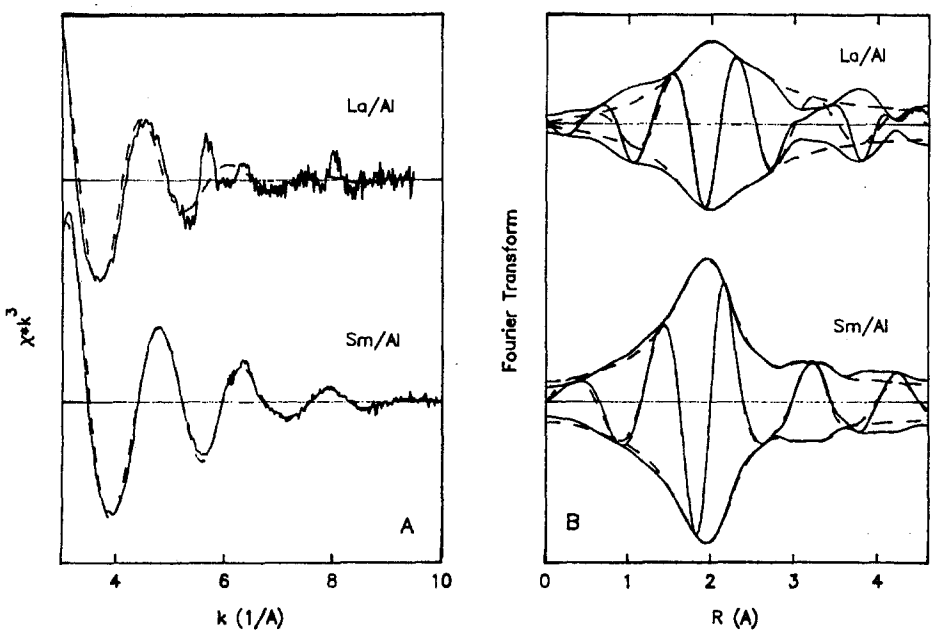

Fig. 9. EXAFS function (A) and FTs (B), at the lanthanide L_{III} edge, for Ln_2O_3/Al_2O_3 supports. Solid lines: unfiltered oscillatory function. Dotted lines: fitted spectra.

Table 5
EXAFS parameter values for Ln_2O_3 and $Ln_2O_3/Al_{22}O_{33}$ samples

	Coordination	N	R (Å)	$\Delta\sigma^2$ (Å^2)
La_2O_3	O	3.8	2.41	0.019
	O	3.0	2.72	0.009
	La	3.0	3.87	0.003
Sm_2O_3	O	3.0	2.38	0.008
	O	3.6	2.64	0.037
	Sm	1.1	3.31	0.008
	Sm	6.0	3.67	0.008
	Sm	4.5	4.18	0.011
$La_2O_3/Al_{22}O_{33}$	O	2.5	2.50	0.011
	O	2.5	2.70	0.015
$Sm_2O_3/Al_{22}O_{33}$	O	3.6	2.43	0.011
	O	5.9	2.65	0.032
	Sm	2.0	3.61	0.018

The absence of aluminum in the coordination shells of the lanthanide cations may indicate either a random distribution of sites or the interaction of the lanthanide cation with hydroxyl groups. This scheme has been proven successful for explaining the structure of Sm_2O_3/Al_2O_3 catalysts as a function of the Sm loading and the calcination temperature [18].

The EXAFS spectra of the catalysts at the L_{III} edge is similar to the one obtained for the supports alone, which may indicate that the catalyst preparation does not influence the structure of the lanthanide supported phase. Again no information is obtained from these spectra on the relative situation of rhodium particles with respect to the lanthanide cations.

However, the dependence of the A_{gem}/A_{lin} ratio on the ionic potential of the lanthanide cation, included in fig. 3, evidences that lanthanide cations are present at the metal–support interface. CO_2 adsorption data also seems to confirm such an hypothesis [7,14].

4. Conclusions

The presence of gem-dicarbonyl species on supported rhodium catalysts seems to be controlled by the surface OH acidity. On doping the support with lanthanide cations the acidity of the surface OH groups is decreased and the relative amount of gem-species decreases.

The lanthanide promoted rhodium catalysts consist of rhodium clusters of increasing size on decreasing the CO/100Rh ratio. Particles, for the more disperse

systems, of 15–20 atoms can be deduced from EXAFS experiments. This model fits fairly well the results obtained from CO chemisorption.

The selectivity towards methane in the hydrogenation of carbon oxides decreases on increasing the metallic dispersion. The modification of metal dispersion is the main effect of the lanthanide promoters.

Acknowledgement

Financial support for this project has been obtained from Comision Interministerial de Ciencia y Tecnologia (PB88-0257 and PB89-0642). JJB and MAC thank the Junta de Andalucia and MJC the Spanish Ministerio de Educacion y Ciencia for the fellowships for obtaining their PhD degrees. We also thank Professor Koningsberger for his help in providing the EXAFS data treatment program and support in the data gathering.

References

[1] G. van der Lee and V. Ponec, Catal. Rev. 29 (1987) 183.
[2] V. Ponec, Stud. Surf. Sci. Catal. 64 (1991) 117.
[3] J.S. Rieck and A.T. Bell, J. Catal. 96 (1985) 88.
[4] S. Bernal, F.J. Botana, R. García and J.M. Rodríguez-Izquierdo, Stud. Surf. Sci. Catal. 48 (1989) 117.
[5] J.A.B. Bourzutschky, N. Homs and A.T. Bell, J. Catal. 124 (1990) 73.
[6] J. Barrault and A. Alouche, Appl. Catal. 58 (1990) 255.
[7] J.A. Odriozola, I. Carrizosa and R. Alvero, Stud. Surf. Sci. Catal. 48 (1989) 713.
[8] R. Kieffer, A. Kiennemann and M. Rodríguez, Appl. Catal. 42 (1988) 77.
[9] J.J. Benítez, R. Alvero, I. Carrizosa and J.A. Odriozola, Catal. Today 9 (1991) 53.
[10] J.J. Benítez, R. Alvero, M.J. Capitan, I. Carrizosa and J.A. Odriozola, Appl. Catal. 71 (1991) 219.
[11] S. Ichikawa, H. Poppa and M. Boudart, J. Catal. 91 (1985) 1.
[12] D.L. Doering, H. Poppa and J.Y. Dickinson, J. Catal. 73 (1982) 104.
[13] J.S. Ledford, M. Houalla, A. Proctor and D.M. Hercules, J. Phys. Chem. 93 (1989) 6770.
[14] R. Alvero, A. Bernal, I. Carrizosa and J.A. Odriozola, Inorg. Chim. Acta 140 (1987) 45.
[15] Y. Mori, T. Mori, T. Hattori and Y. Murakami, Appl. Catal. 59 (1990) 66.
[16] R. Alvero, A. Bernal, I. Carrizosa, J.A. Odriozola and J.M. Trillo, Appl. Catal. 25 (1986) 207.
[17] G. Gallaher, J.G. Goodwin Jr., C.S. Huang and M. Houalla, J. Catal. 127 (1991) 719.
[18] M.J. Capitan, P. Malet, M.A. Centeno, A. Munoz-Perez, I. Carrizosa and J.A. Odriozola, J. Phys. Chem., submitted.
[19] A.G. McKale, B.W. Veal, A.P. Paulikas, S.K. Chan and G.S. Knapp, J. Am. Chem. Soc. 110 (1988) 3763.
[20] F.W.H. Kampers and D.C. Koningsberger, Faraday Discussions Chem. Soc. 87 (1990) 137.
[21] L. Guczi, in: *New Trends in CO Activation*, ed. L. Guczi (Elsevier, Amsterdam, 1991) p. 350.
[22] J. Read, Can. J. Chem. 50 (1972) 490.
[23] A. Crucq, L. Degols, A. Frennet and G. Lienard, Catal. Today 5 (1989) 223.
[24] R.R. Cavanagh and J.T. Yates Jr., J. Chem. Phys. 74 (1981) 4150.

[25] R. Alvero, I. Carrizosa, J.A. Odriozola, J.M. Trillo and S. Bernal, J. Less-Common Met. 94 (1983) 139.
[26] J.L.G. Fierro, J. Soria, J. Sanz and J.M. Rojo, J. Solid State Chem. 66 (1987) 154.
[27] B.E. Koel and G.A. Somorjai, in: *Catalysis Science and Technology*, Vol. 7, eds. J.R. Anderson and M. Boudart (Springer, Berlin, 1985) p. 159.
[28] L.M. Hamadeh and P.R. Griffiths, Appl. Spectry. 41 (1987) 682.
[29] W.M.H. Sachtler and M. Ichikawa, J. Phys. Chem. 90 (1986) 4752.
[30] J.P. Hindermann, A. Kiennemann and S. Tazkritt, Stud. Surf. Sci. Catal. 48 (1989) 481.
[31] D.G. Castner, L.H. Dubois, B.A. Sexton and G.A. Somorjai, Surf. Sci. 103 (1981) L134.
[32] A. Erdohelyi and F. Solymosi, J. Catal. 84 (1983) 446.
[33] C.A. Rice, S.D. Worley, C.W. Curtis, J.A. Guin and A.R. Tarrer, J. Chem. Phys. 74 (1981) 6487.
[34] H.F. van 't Blik, J.B.A.D. van Zon, J.C. Vis, D.C. Koningsberger and R. Prins, J. Phys. Chem. 87 (1983) 2264.
[35] F. Solymosi and M. Pasztor, J. Phys. Chem. 89 (1985) 4789.
[36] D.K. Paul and J.T. Yates Jr., J. Phys. Chem. 95 (1991) 1699.
[37] T.M. Duncan, J.T. Yates Jr. and R.W. Vaughan, J. Chem. Phys. 73 (1980) 975.
[38] T.H. Ballinger and J.T. Yates Jr., J. Phys. Chem. 95 (1991) 1694.
[39] T. Hattori, S. Komai, E. Nagata and Y. Murakami, J. Catal. 127 (1991) 460; M.A. Vannice and C.C. Twu, J. Chem. Phys. 75 (1981) 5944.
[40] L.H. Dubois and G.A. Somorjai, in: *Vibrational Spectroscopies for Adsorbed Species*, eds. A.T. Bell and M.L. Hair (The American Chemical Society, Washington, 1980) p. 163.
[41] D.G. Castner and G.A. Somorjai, Surf. Sci. 83 (1979) 60.
[42] B.A. Sexton and G.A. Somorjai, J. Catal. 46 (1977) 167.
[43] G.A. Somorjai, J.E. Crowell and W.T. Tysoe, J. Phys. Chem. 89 (1986) 1598.
[44] H.P. Bonzel, Surf. Sci. 226 (1990) 237.
[45] K. Tamura and Y. Nihei, J. Catal. 115 (1989) 273.